Possible Oxidative Polymerization Mechanism of 5,6-Dihydroxyindole from ab Initio Calculations

Hidekazu Okuda*

Integrative Bioscience and Biomedical Engineering, Waseda University, Shinjuku, Tokyo 169-8555, Japan

Kazumasa Wakamatsu and Shosuke Ito

Department of Chemistry, Fujita Health University School of Health Sciences, Toyoake, Aichi 470-1192, Japan

Takayuki Sota

Department of Electrical Engineering and Bioscience, Waseda University, Shinjuku, Tokyo 169-8555, Japan

Received: November 20, 2007; Revised Manuscript Received: April 23, 2008

The reactivity of 5,6-dihydroxyindole and its major dimers has been studied with the use of a recently proposed general-purpose reactive indicator (Anderson et al. *J. Chem. Theory Comput.* **2007**, *3*, 358−374) from ab initio density-functional theory calculations. Theoretical prediction has reasonably explained previously isolated oligomers up to tetramers. The oxidative polymerization is governed by the electron-transfer-controlled reaction. The electrostatic interaction plays a regioselective role in the reactant complex and/or intermediates. A monomer−dimer coupling is able to form trimers, while a part of it is prevented by the exchange repulsion, i.e., steric hindrance. Therefore, a dimer−dimer coupling is also able to form tetramers.

1. Introduction

It is widely believed that eumelanin, a brown-to-black pigment, provides photoprotection and shields epidermal cells from radiation in the ultraviolet (UV) and visible (VIS) frequency regions. 5,6-Dihydroxyindole (DHI, **1** in Figure 1), 5,6-dihydroxyindole-2-carboxylic acid (DHICA), and their oxidized molecules are considered as the precursors of eumelanin, and their polymerization seems to produce eumelanin, but the chemical structure of eumelanin is not well understood.[1−9]

Some properties of eumelanin were explained[9] by considering semiconductor model.[10] For example, the optical absorption of eumelanin, which is the well-known broad absorption and looks like an inorganic material, was considered to give support to this model.[11] It was also shown that eumelanin can act as the electrical switch.[12] It was also demonstrated that the broad absorption spectrum was explained naturally based on a chemical disorder model.[13,14] In the model eumelanin is considered as an ensemble of chemically distinct oligomeric macromolecules with an individual optical gap.[14] Therefore understanding polymerization mechanism of the precursors of eumelanin is important.

The precise mechanism of oxidative coupling of **1** and of DHICA remains unclear. To analyze the oxidative polymerization mechanism, many experimental efforts have been made to isolate oligomers.[15−20] With respect to oligomers consisting of **1**, Naples' group clarified the early stages of the polymerization process of **1** up to tetramers (Figure 1).[16,17,19,20] These oligomers were isolated as acetyl derivatives and all oligomers mentioned above have a single linkage.

At the dimer level, the 2,4′-, 2,7′-, and 2,2′-biindolyls, **2**, **3**, and **4**, were isolated.[16,17] Note that the 2,2′-linked homodimer **4** is produced only in the presence of the transition-metal cations (e.g., Ni^{2+} and Zn^{2+}).[16] It was suggested from product analysis that the process involves the nucleophilic attack of a dihydroxyindole to one of its two-electron-oxidants as an electrophile. DHI homotrimers were also isolated as 2,4′:2′,4″- and 2,4′:2′,7″-terindolyls (**5** and **6**) in the process of oxidation of **1**.[17] The structural features of oligomers up to trimers showed that the coupling through the 2,4′- and 2,7′-linkages is preferable. Thus, product analysis had disproved the mode of polymerization of **1** via the C3 position proposed earlier,[17] and so it was a surprise for Naples' group to isolate the tetramer, 5,5′,5″,5‴,6,6′,6″,6‴-octahydroxy-2,4′:2′,3″:2″,4‴-tetraindolyl **7** with unexpected 2,3′-coupling, in the process of the oxidation of **2** in the presence of Zn^{2+} ion.[19] Furthermore, the additional anomalous linkages, 3,3′ and 4,4′, were found in the oxidation of **3**: 7,2′:3′,3″:2″,7‴-, 2,7′:4′,4″:7″,2‴-, and 2,7′:2′,3″:2″,7‴-tetraindolyls (**8**, **9**, and **10**) are isolated.[20] The group also showed that **10** becomes preferable enough to be one of the major products by the influence of Zn^{2+} ion.[20]

Ab initio studies have been started on oligomers consisting of **1** and/or DHICA to clarify their electronic structures and the UV−vis spectra.[13,21−24] However, in all of those studies oligomer structures have been assumed a priori according to chemical speculation. This is because, to the best of our knowledge, even the reactivity of **1** and/or DHICA monomers has not been studied from ab initio calculations. Quite recently, Anderson et al.[25] proposed a general-purpose reactive indicator for nucleophiles and electrophiles. The indicator is considered to be useful because it can describe not only electrostatic-controlled reactions and electron-transfer-controlled reactions but also reactions between these extreme reactions.

In this paper, we examine the oxidative polymerization mechanism of **1** with the general-purpose reactive indicator from ab initio density-functional theory calculations. We demonstrate that the oxidative polymerization mechanism of **1** is governed by the electron-transfer-controlled reaction at least up to the

* Corresponding author. Tel: +81-3-5286-3378. Fax: +81-3-3207-1488. E-mail: h.okuda@asagi.waseda.jp.

10.1021/jp711025m CCC: $40.75
Published on Web 10/14/2008

formation of tetramers. The electrostatic interaction has been suggested to play a regioselective role in the reactant complex and/or in the intermediate. A monomer−dimer coupling is able to form trimers, while a part of it is prevented by the exchange repulsion, i.e., steric hindrance. Therefore, a dimer−dimer coupling is also able to form tetramers.

2. Details of Calculations

All ab initio density-functional theory (DFT) calculations[26,27] have been carried out using the B3LYP functional,[28] which consists of Becke's exchange functional and the slightly modified Lee−Yang−Parr correlation functional. We have used the 6-31++G(d,p) basis set,[29,30] which takes account of diffuse functions for all atoms and d polarization functions on heavy atoms and p polarizations on hydrogen atoms. The solvent effect has been taken into account by the polarizable continuum model.[31] The CHelpG method[32] has been used for estimating the effective point charge on each atom. Harmonic vibrational wavenumbers have been calculated analytically and scaled by 0.982. The excitation energy of each molecule has been estimated by the time-dependent DFT (TD-DFT) with the B3LYP functional and 6-31++G(d,p) basis set to verify optimized molecular structures in comparison with previous results. All ab initio calculations have been carried out using the Gaussian 03 program.[33]

In order to evaluate the reactivity of molecules, we have used the indicators proposed by Anderson et al.[25] They derived the indicators by considering both electron-transfer effects and electrostatic interactions. The indicator for nucleophiles is given by

$$\Xi^{\kappa}_{\Delta N\le 0,\alpha} = (\kappa+1)q^{(0)}_{\alpha} - \Delta N(\kappa-1)f^{-}_{\alpha} \quad (1)$$

and that for electrophiles is given by

$$\Xi^{\kappa}_{\Delta N\ge 0,\alpha} = -(\kappa+1)q^{(0)}_{\alpha} + \Delta N(\kappa-1)f^{+}_{\alpha} \quad (2)$$

Here, subscript α specifies the reactive position, and $q^{(0)}_{\alpha}$ and $f_{\alpha}{}^{\pm}$ denote the effective point charge and condensed Fukui functions, respectively, on the reactive position α. The condensed Fukui functions on the reactive position α are defined as

$$f^{-}_{\alpha} = q^{(-)}_{\alpha} - q^{(0)}_{\alpha} \quad (3)$$

$$f^{+}_{\alpha} = q^{(0)}_{\alpha} - q^{(+)}_{\alpha} \quad (4)$$

In the equations, $q^{(-)}_{\alpha}$ and $q^{(+)}_{\alpha}$ denote the effective point charge for the radical cation of the nucleophile without a transferring electron and that for the radical anion of the electrophile with an additional electron, respectively. (Although in the original papers by Anderson et al.[25] the expressions of $q^{(0)}_{\text{nucleophile},\alpha}$, $q^{(0)}_{\text{electrophile},\alpha}$, $q^{(-)}_{\text{nucleophile},\alpha}$, $q^{(+)}_{\text{electrophile},\alpha}$, $f^{-}_{\text{nucleophile},\alpha}$, and $f^{+}_{\text{electrophile},\alpha}$ are used, the subscripts "nucleophile" and "electrophile" are omitted in this paper since they are understood from the superscripts.) In calculating $q^{(0)}_{\alpha}$ and $q^{(\pm)}_{\alpha}$, they pointed out that the effective point charge on the reactive position α should include that on the adjacent hydrogen atom. Equations 1 and 2 include the two parameters, ΔN and κ. The parameter ΔN denotes the amount of electron transfer in the reaction and can be calculated from ab initio calculations. The other parameter κ describes the chemical reaction type and should be treated as a variable: $\kappa > 1$, strong electrostatic control; $\kappa = 1$, pure electrostatic control; $-1 < \kappa < 1$, joint control by electrostatics and electron-transfer effects; $\kappa = -1$, pure electron-transfer control; $\kappa < -1$, strong electron-transfer control. Since $\Xi^{\kappa}_{\Delta N,\alpha}$ models the interaction energy of the molecule, the most reactive position of the molecule is the reactive position with the most negative $\Xi^{\kappa}_{\Delta N,\alpha}$.

3. Results and Discussion

3.1. Reactivity of Monomers. The molecular structures of **1** and **11** (see Figure 2) were optimized in aqueous solution. The excitation energy of each molecular structure was calculated by using TD-DFT. The results are essentially identical to those reported previously[34] (see the Supporting Information), validating our structure calculations. We summarized the energy of the highest occupied molecular orbital (HOMO) ($\varepsilon_{\text{HOMO}}$) and that of the lowest unoccupied molecular orbital (LUMO) ($\varepsilon_{\text{LUMO}}$) for **1** and **11** in Table 1. The relation $\varepsilon_{\text{HOMO},\mathbf{11}} < \varepsilon_{\text{HOMO},\mathbf{1}} < \varepsilon_{\text{LUMO},\mathbf{11}} < \varepsilon_{\text{LUMO},\mathbf{1}}$ holds (subscripts **1** and **11** specify the molecules). This means that **1** acts as a nucleophile and **11** as an electrophile in the dimerization process as suggested previously.[8] We calculated the energy difference $\Delta\varepsilon$ between $\varepsilon_{\text{LUMO}}$ for the electrophile and $\varepsilon_{\text{HOMO}}$ for the nucleophile since the reaction is easy to occur with the small $\Delta\varepsilon$. No significant difference in $\Delta\varepsilon$ (see Figure 3) suggests that any of the reactions occurs similarly.

As the probability of reaction is also proportional to the collision rate between the target molecule and the other one in the reactant complex, we calculated the probability of finding each conformer **1** and tautometer **11** in aqueous solution using the Boltzmann factor, which depends on both temperature and the relative energy difference in conformers/tautomers. The relative energy difference was estimated using the dissociation energy, which is defined as the sum of the binding energy and the vibrational zero-point energy. The temperature was set to be 300 K. It was found from Table 1, in which the probability of finding each conformer **1** and tautometer **11** is also tabulated, that **1** should exist as a mixture of at least three conformers and the probabilities of finding **11b** and **11c** were negligibly small in comparison with that of finding **11a**. This agrees with the previous result.[34] Hence we focus our attention on the dimerization reaction of **1** against **11a** hereafter.

Only carbons on 2, 3, 4, and 7 positions, i.e., C2, C3, C4, and C7 positions in abbreviated representations, were treated as reactive positions. The effective point charge on each reactive position of **1** and **11a** is tabulated in Table 2, where the condensed Fukui function and reactivity indicator under the condition of $\kappa = -1$ and $|\Delta N| = 1$ are also shown (for **11b** and **11c**, see the Supporting Information). The effective point charge on each carbon includes that on the adjacent hydrogen atom.[25] It is found from Table 2 that the C2 positions are positively charged and the other reactive positions are negatively charged for both **1** and **11a**. It is likely that Coulomb repulsion prevents the C2 positions of **1** and **11a** from facing and approaching each other in the reactant complex. Taking account of Coulomb attraction, there are two possible reaction paths: (i) The C2 position of **1** attacks one of the C3, C4, and C7 positions of **11a**; (ii) The C2 position of **11a** attacks one of the C3, C4, and C7 positions of **1**.

To identify theoretically which path is favorable, we should first estimate $\Xi^{\kappa}_{\Delta N,\text{C2}}$ for **1** and **11a**. As mentioned before, $\Xi^{\kappa}_{\Delta N,\alpha}$ includes two parameters ΔN and κ. The electronic structure of each monomer and possible dimer in aqueous solution is such that the amount of electron transfer from **1** to **11a** in the dimerization reaction almost equals unity ($|\Delta N| \sim 1$), which is retained in any possible dimerizations, i.e., producing the 2,2′-, 2,4′-, or 2,7′-biindolyl independent of the reaction paths (i) and (ii). As mentioned in the original paper by Anderson et al.,[25]

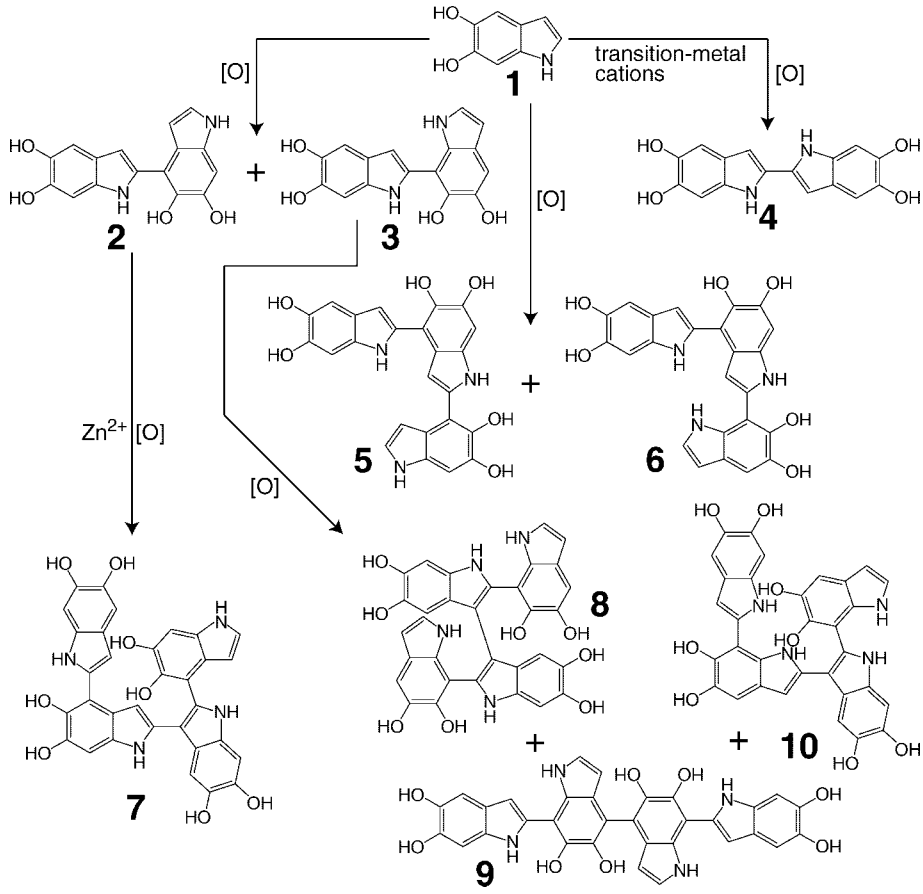

Figure 1. Oligomers isolated by oxidation of **1** (refs 16, 17, 19, and 20).

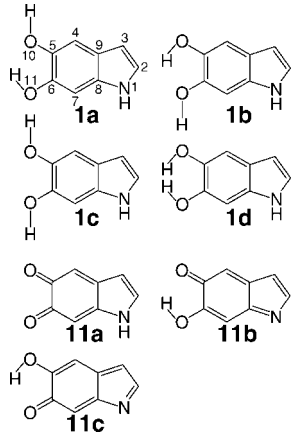

Figure 2. Structural formulas for conformers of **1** (**1a**−**1d**), indolequinone (IQ, **11a**), quinonimine (**11b**), and quinone methide (**11c**). The numbers 1−11 in **1a** are the labels of the atoms, to which the labels for **1b**−**1d** and **11** are identical. We consider the C2, C3, C4, and C7 positions as reactive positions.

the parameter ΔN is exactly evaluated from ab initio calculations, see the Supporting Information. Therefore, we can safely set $|\Delta N| = 1$ in calculating $\Xi^{\kappa}_{\Delta N,\alpha}$ for the present system.

Ideally, $|\Delta N| = 1$ should result that the dimerization reaction is the electron-transfer-controlled reaction and the other parameter κ should be simultaneously $\kappa = -1$.[25] We have shown $\Xi^{\kappa=-1}_{|\Delta N|=1,\alpha}$ of each reactive position α in Table 2. As for the κ-dependence of $\Xi^{\kappa}_{|\Delta N|=1,\alpha}$ in the range of $-1 \le \kappa \le 1$, see the Supporting Information. Under the condition of $|\Delta N| = 1$ and $\kappa = -1$, it is found that $\Xi^{\kappa=-1}_{\Delta N=-1,C2} = -0.4060$ for **1a**, $\Xi^{\kappa=-1}_{\Delta N=-1,C2} = -0.4706$ for **1b**, $\Xi^{\kappa=-1}_{\Delta N=-1,C2} = -0.4433$ for **1c**, $\Xi^{\kappa=-1}_{\Delta N=-1,C2} = -0.4608$ for **1d**, and $\Xi^{\kappa=-1}_{\Delta N=1,C2} = -0.2889$ for **11a**. Although the original paper by Anderson et al.[25] just states that "a molecule is most reactive in the places where $\Xi^{\kappa}_{\Delta N}(r)$ (defined as $\Xi^{\kappa}_{\Delta N}(r) \approx \Sigma_{\alpha}\Xi^{\kappa}_{\Delta N,\alpha}(r)/|r - R_{\alpha}|$) is the most negative", we stretch the meaning of $\Xi^{\kappa}_{\Delta N,\alpha}$ such that the reactive position with the most negative $\Xi^{\kappa}_{\Delta N,\alpha}$ may be most reactive even when two different molecules are compared with each other. So we interpret that the C2 position of **1b** is the key reactive position in the dimerization and the reaction path (i) is favorable. As $\Xi^{\kappa=-1}_{|\Delta N|=1,\alpha} = -2f^{\pm}_{\alpha}$, the most negative $\Xi^{\kappa=-1}_{\Delta N=-1,C2}$ means the most positive f^{-}_{C2}. This indicates that the C2 position of **1b** has the highest electron-donating capability.

Remembering that Coulomb repulsion prevents the reaction from forming the 2,2′-linkage, the most reactive position of **11a** is found to be the C4 position with $\Xi^{\kappa=-1}_{\Delta N=1,C4} = -0.2086$ and the next-most reactive position is the C7 position with $\Xi^{\kappa=-1}_{\Delta N=1,C7} = -0.1863$. The reactivity of the C3 position of **11a** is extremely low in comparison with the other two positions judging from $\Xi^{\kappa=-1}_{\Delta N=1,C3} = -0.0299$. These results predict that the 2,4′-biindolyl **2** is the primary product, the 2,7′-biindolyl **3** is the secondary one, and the 2,3′-biindolyl is hardly produced. The small f^{+}_{C3} means that the C3 position of **11a** has little electron-accepting capability. The same order of products holds in the parameter region of $-1 \le \kappa < 0.77$ (see the Supporting Information). Almost the same holds for the reaction between **1a**, **1b**, or **1d** and **11a**. Theoretical prediction on the formation of dimers is schematically summarized in Figure 4.

Another reaction picture may be possible when intermediates are considered. We tentatively call it a radical ion picture. As already mentioned $q^{(-)}_{\alpha}$ ($q^{(+)}_{\alpha}$) is the effective point charge on each reactive position α after one electron transfer from **1** to **11** and, therefore, is regarded as the effective point charge of a radical cation (anion). In the intermediate state of the reaction of **1** against **11a**, the largest Coulomb attraction acting between

TABLE 1: Energies of HOMO and LUMO for 1 and 11[a] and Probabilities of Finding Conformers of 1 and Tautomers of 11[b]

	1a	1b	1c	1d	11a	11b	11c
ε_{HOMO}	−5.4072	−5.4372	−5.3843	−5.4417	−5.8996	−6.1899	−6.2845
ε_{LUMO}	−0.4934	−0.4889	−0.4659	−0.5270	−3.7468	−3.9531	−3.8541
probability	44.27	37.31	17.79	0.62	100.00	1.24×10^{-8}	1.80×10^{-5}

[a] In units of eV. [b] In units of %.

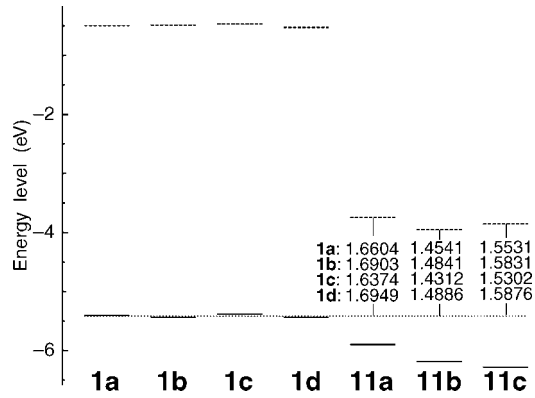

Figure 3. Energy level scheme of HOMO (horizontal solid line) and LUMO (horizontal dashed line) for **1** and **11**. The energy differences between $\varepsilon_{HOMO,1}$ and $\varepsilon_{LUMO,11}$ are also shown. This scheme indicates that (i) **1a**−**1d** are almost identical to each other at least energetically, (ii) **1** acts as a nucleophile and **11** acts as an electrophile, and (iii) changes in these possible reactions are not so significant.

TABLE 2: Effective Point Charges,[a] Condensed Fukui Function,[a] and Reactive Indicator[b] on Each Reactive Position for 1 and 11[c]

		C2	C3	C4	C7
1a	$q_\alpha^{(0)}$	0.0819	−0.2080	−0.2844	−0.1671
	$q_\alpha^{(-)}$	0.2849	−0.0423	−0.1488	−0.1016
	f_α^-	0.2030	0.1656	0.1356	0.0655
	$\Xi_{\Delta N=-1,\alpha}^{\kappa=-1}$	−0.4060	−0.3313	−0.2713	−0.1310
1b	$q_\alpha^{(0)}$	0.0721	−0.1796	−0.2314	−0.2163
	$q_\alpha^{(-)}$	0.3074	−0.0728	−0.1416	−0.1520
	f_α^-	0.2353	0.1068	0.0898	0.0644
	$\Xi_{\Delta N=-1,\alpha}^{\kappa=-1}$	−0.4706	−0.2136	−0.1796	−0.1287
1c	$q_\alpha^{(0)}$	0.0693	−0.1955	−0.3001	−0.2159
	$q_\alpha^{(-)}$	0.2910	−0.0927	−0.2302	−0.1557
	f_α^-	0.2216	0.1028	0.0699	0.0603
	$\Xi_{\Delta N=-1,\alpha}^{\kappa=-1}$	−0.4433	−0.2055	−0.1398	−0.1205
1d	$q_\alpha^{(0)}$	0.0714	−0.1720	−0.2111	−0.1127
	$q_\alpha^{(-)}$	0.3018	−0.0311	−0.0687	−0.0607
	f_α^-	0.2304	0.1409	0.1424	0.0520
	$\Xi_{\Delta N=-1,\alpha}^{\kappa=-1}$	−0.4608	−0.2818	−0.2849	−0.1041
11a	$q_\alpha^{(0)}$	0.1980	−0.1415	−0.2811	−0.2159
	$q_\alpha^{(+)}$	0.0531	−0.1564	−0.3854	−0.3090
	f_α^+	0.1449	0.0149	0.1043	0.0932
	$\Xi_{\Delta N=1,\alpha}^{\kappa=-1}$	−0.2899	−0.0299	−0.2086	−0.1863

[a] In units of elementary charge. [b] Under the condition of $|\Delta N| = 1$ and $\kappa = -1$. [c] See Figure 2 for the labels of the atoms.

the corresponding radicals leads to **2** and the next largest Coulomb attraction leads to **3** (see Table 2).

In any case theoretical prediction is consistent with the previous product analysis in the absence of transition-metal cations. That is, **2** is the primary product, **3** is the secondary one, and the other dimers were not isolated.[17] Note that the relative yield of **2** and **3** depends on the reaction conditions and **3** may become a primary product in several conditions.[23]

It should be noted here that when the other possible reaction path (ii) is selected, the theoretical prediction contradicts the experimental results.[17] This fact appears to validate a broad interpretation of $\Xi_{\Delta N,\alpha}^{\kappa}$ mentioned before.

We briefly consider the dimerization mechanism in the presence of transition-metal cations. It is natural to consider

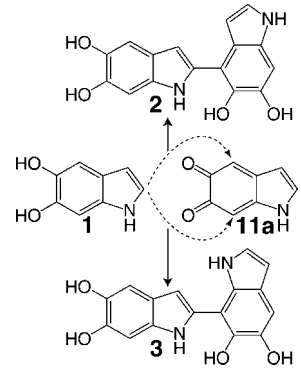

Figure 4. Proposed origin of the formation of 2,4′- and 2,7′-biindolyls. The nucleophilic attack of the C2 position of **1** to the C4 and C7 positions of **11a** leads to **2** and **3**, respectively.

that transition-metal cations might prevent Coulomb attraction from acting between the C2 position of **1** and the C4 and C7 positions of **11a**. Analysis of the reason is beyond the scope of this paper and we do not discuss it further. Nevertheless, the 2,2′-linkage may be formed under such a circumstance because the reactivity of the C2 positions of both **1** and **11a** is essentially high (see Table 2).

3.2. Reactivity of Dimers. In the following, we discuss the reactivity of **1**-related dimers which appear to take part in the formation of trimers and tetramers. From the discussion for **1**-related monomers mentioned above, it is certain that the polymerization of **1** is the electron-transfer-controlled reaction and the electrostatic interaction plays the regioselective role. We consider the formation mechanism of **5**−**7** in this section. Furthermore, we predict possible tetramers via the coupling of **3** and its two-electron-oxidant. Note that we do not distinguish **1a**−**1d** from each other in this section because the four molecules are essentially identical to each other in terms of the HOMO and LUMO energies and the reactivity (see the previous section), and we use **1a** as a typical molecule in the discussion below.

***3.2.1. Formation Mechanism of 2,4′:2′,4″-Terindolyl* 5.** Both 5,5′,5″,6,6′,6″-hexahydroxy-2,4′:2′,4″- and 2,4′:2′,7″-terindolyls (**5** and **6**) were isolated experimentally without transition-metal cations.[17] We start from considering the formation mechanism of the former. There are two possible pathways to form **5**: One is a reaction of **1** against one of two-electron-oxidants of **2** and the other is a reaction of **2** against **11**. As already mentioned in the previous section, the C2 position of **1** is the most reactive among possible reactive positions of **1** and **11**. It is reasonable to consider that the C2 position of **1** is the key reactive position even in forming trimers and so the other molecule participating in the reaction is one of two-electron-oxidants of **2**. Exclusion of the latter pathway is justified later. Hence we optimized the molecular structures of four tautomers/conformers of the two-electron-oxidants of **2** in aqueous solution from the viewpoint of stability, i.e., extended quinone methide with geometry *Z* **12a** (**3a**), that with geometry *E* **12b** (**3e**), 2-substituted quinone with syn-periplanar (*sp*) symmetry **12c** (**3p**), and 2-substituted methide with *sp* symmetry **12d** (**3i**) (see

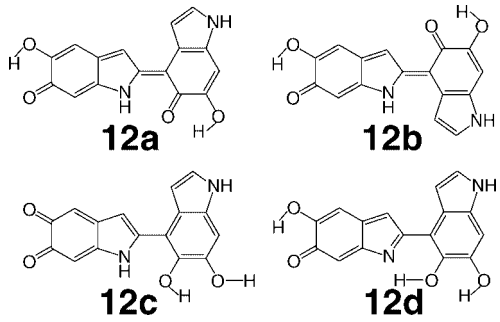

Figure 5. Structural formula of **12**, two-electron-oxidants of **2**, under consideration.

TABLE 3: Energies of HOMO and LUMO for 12[a] and Probabilities of Finding Tautomers 12[b]

	12a	12b	12c	12d
ε_{HOMO}	−5.3951	−5.3718	−5.5519	−5.6692
ε_{LUMO}	−3.7477	−3.7121	−3.6338	−3.7815
probability	98.57	1.42	1.26×10^{-2}	2.50×10^{-4}

[a] In units of eV. [b] In units of %.

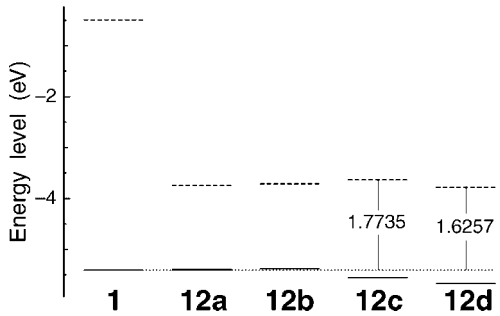

Figure 6. Energy level scheme of HOMO (horizontal solid line) and LUMO (horizontal dashed line) for **1** and **12**. The energy differences between $\varepsilon_{HOMO,1}$ and $\varepsilon_{LUMO,12c}$ and $\varepsilon_{LUMO,12d}$ are also shown. This scheme indicates that **1** hardly reacts with **12a** and **12b** due to exchange repulsion and reacts as a nucleophile with **12c** and **12d** as electrophiles and that the changes in the reactions of **1** against **12c** and **12d** are not so significant energetically.

Figure 5). Here, symbols in parentheses are those of ref 23. The stability of each molecule was studied with the dissociation energy.

Energy levels of HOMO and LUMO in each oxidant are shown in Table 3 and are compared with those of **1** in Figure 6. In Table 3, the probabilities of finding tautomers **12** are also tabulated. The energy level scheme indicates that the reaction of **1** against the most stable oxidant **12a** cannot be regarded as a reaction of a nucleophile against an electrophile. The extremely small difference in the energy level of each HOMO suggests that **1** hardly reacts with **12a** due to exchange repulsion or Pauli repulsion, which is termed steric hindrance in the field of organic chemistry. Almost the same holds for the reaction of **1** against the next-most stable oxidant **12b** (see Figure 6). The fact that **12a** and **12b** are not consumed in forming trimers makes the formation of tetramers via a dimer−dimer coupling possible and an important reaction mechanism. Such a reaction picture that a nucleophile attacks an electrophile holds for the reactions of **1** against more unstable oxidants, **12c** and **12d**. The probability of finding **12c** is 1.26×10^{-2}% and that of finding **12d** is at most 3×10^{-4}% (see Table 3). Therefore, it is sufficient to consider the reaction of **1** against **12c** the highest priority in clarifying the formation mechanism of **5**.

The effective point charge and condensed Fukui function for each reactive position of **12a**−**12c** are tabulated in Table 4, where the reactive indicator under the condition of $\kappa = -1$ and $\Delta N = 1$ is also shown. Analogous to the formation of dimers, $|\Delta N| = 1$ may be a good approximation even in forming **5**. This is justified by the molecular structure calculation of **5**. As for estimation of ΔN and the κ-dependence of reaction index, see the Supporting Information. The formation of **5** is also suggested as a result of the electron-transfer-controlled reaction and so it is sufficient to consider the limit of $|\Delta N| = 1$ and $\kappa = -1$ primarily. At the limit, the following is found from Tables 2 and 4. The C2 position of **1** is the most reactive among the reactive positions of **1** and **12c**. The C2 position of **1** will attack a reactive position with negative charge and most or more negative $\Xi^{\kappa=-1}_{\Delta N=1,\alpha}$. Such a reactive position is the C4 position on the 2-substituted indole of **12c**. In the radical ion picture, the reaction is interpreted as follows. After an electron transfer from **1** to **12c**, the largest Coulomb attraction acts between the C2 position of **1** and the C4 position on the 2-substituted indole of **12c**. In any way, the nucleophilic attack of the C2 position of **1** to the C4 position on the 2-substituted indole of **12c** leads to **5**.

***3.2.2. Formation Mechanism of 2,4′:2′,7″-Terindolyl* 6.** Here we discuss the formation of 5,5′,5″,6,6′,6″-hexahydroxy-2,4′:2′,7″-terindolyl **6**. Although the reaction of **2** against **11** and that of **1** against **12** can form **6**, we consider the reactions of **1** against two-electron-oxidants of **3** analogous to the formation of **5**.

We considered the reactions of **1** against five tautomeric/conformeric two-electron-oxidants of **3**, i.e., extended quinone methide with geometry *Z* **13a** (**4a**), that with geometry *E* **13b** (**4e**), 2-substituted quinone with *sp* symmetry **13c** (**4o**), that with antiperiplanar (*ap*) symmetry **13d** (**4q**), and 2-substituted methide with *sp* symmetry **13e** (**4j**) (see Figure 7). Here, symbols in parentheses are those of ref 23. The HOMO and LUMO energies of **13** are summarized in Table 5, and the energy scheme of **13** is compared with that of **1** in Figure 8. In Table 5 the probabilities of finding tautomers **13** are also tabulated. It may be concluded from Table 5 and Figure 8 that **1** hardly reacts with **13a** and **13b** due to exchange repulsion. Therefore, we consider the reaction of **1** against the third and fourth stable molecules, **13c** and **13d**, which may act as electrophiles for **1**. Note that we may neglect the fifth stable molecule **13e** because the probability of finding **13e** is much less than those of finding **13c** and **13d** (see Table 5).

The effective point charge, condensed Fukui function, and reactive indicator under the condition of $\kappa = -1$ and $\Delta N = 1$ for each reactive position of **13a**−**13d** are tabulated in Table 6. As for estimation of ΔN and the κ-dependence of reaction index, see the Supporting Information. The approximation $|\Delta N| = 1$ appears to be appropriate again in the formation of **6** and so it may be sufficient to consider the limit of $|\Delta N| = 1$ and $\kappa = -1$ primarily. At the limit, the following is found from Tables 2 and 6. The C2 position of **1** is the most reactive among the reactive positions of **1**, **13c**, and **13d**. Regarding the C2 position of **1** as the key reactive position, we looked for a reactive position with the most negative $\Xi^{\kappa=-1}_{\Delta N=1,\alpha}$ in **13c** and **13d**. For **13c** (**13d**), the C7 (C4) position on the 2 (7)-substituted indole has the most negative $\Xi^{\kappa=-1}_{\Delta N=1,\alpha}$. Resultant products are 2,7′:2′,7″-terindolyl from the reaction of **1** against **13c** and 2,4′:7′,2″-terindolyl from the reaction of **1** against **13d**. However, such trimers were not isolated experimentally.[17] The inconsistency is not easily resolved even when the energy of reaction complex is additionally taken into account.

There is no inconsistency between the theoretical prediction and the product analysis when the radical ion picture is used.

TABLE 4: Effective Point Charges,[a] Condensed Fukui Function,[a] and Reactive Indicator[b] on Each Reactive Position for 12a−12c

		C3	C4	C7	C2′	C3′	C7′
12a	$q_\alpha^{(0)}$	− 0.0967	− 0.1233	− 0.2463	0.1003	− 0.1575	− 0.0347
	$q_\alpha^{(+)}$	− 0.2298	− 0.1753	− 0.2948	0.0590	− 0.1849	− 0.1250
	f_α^+	0.1332	0.0520	0.0485	0.0413	0.0274	0.0903
	$\Xi_{\Delta N=1,\alpha}^{\kappa=-1}$	−0.2664	−0.1040	−0.0969	−0.0826	−0.0549	−0.1806
12b	$q_\alpha^{(0)}$	− 0.0534	− 0.1314	− 0.2260	0.0944	− 0.1312	− 0.0512
	$q_\alpha^{(+)}$	− 0.1422	− 0.1694	− 0.2722	0.0579	− 0.1564	− 0.1341
	f_α^+	0.0888	0.0380	0.0462	0.0365	0.0251	0.0829
	$\Xi_{\Delta N=1,\alpha}^{\kappa=-1}$	−0.1776	−0.0760	−0.0925	−0.0730	−0.0502	−0.1658
12c	$q_\alpha^{(0)}$	− 0.2332	− 0.2810	− 0.2433	0.1347	− 0.1798	− 0.1331
	$q_\alpha^{(+)}$	− 0.2559	− 0.3492	− 0.2878	0.0653	− 0.1520	− 0.1645
	f_α^+	0.0226	0.0682	0.0444	0.0694	− 0.0277	0.0314
	$\Xi_{\Delta N=1,\alpha}^{\kappa=-1}$	−0.0453	−0.1364	−0.0889	−0.1389	0.0555	−0.0628

[a] In units of elementary charge. [b] Under the condition of $\Delta N = 1$ and $\kappa = -1$.

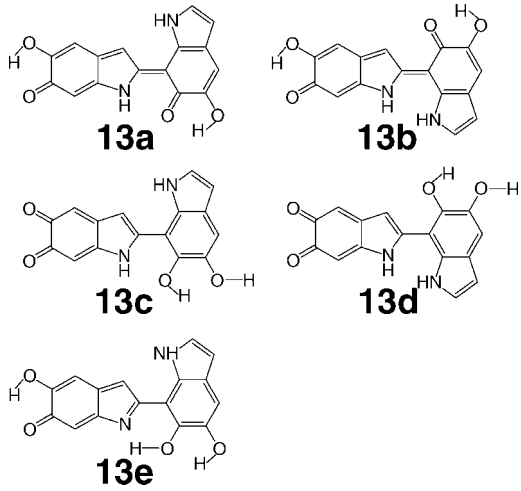

Figure 7. Structural formula of **13**, two-electron-oxidants of **3**, under consideration.

TABLE 5: Energies of HOMO and LUMO for 13[a] and Probabilities of Finding Tautomers 13[b]

	13a	13b	13c	13d	13e
ε_{HOMO}	−5.4121	−5.3849	−5.6294	−5.6060	−5.7344
ε_{LUMO}	−3.7846	−3.7543	−3.6711	−3.6638	−3.8309
probability	96.97	2.99	2.65×10^{-2}	1.22×10^{-2}	8.74×10^{-5}

[a] In units of eV. [b] In units of %.

The C2 position of the radical cation of **1** is still the most reactive in the sense that it has the most positive charge. The most reactive positions against it are the C4 positions on the 2-substituted indoles for the radical anions of **13c** and **13d**, because the positions have the most negative charge among the reactive positions of **13c** or **13d**. Therefore, the primary resultant trimer is **6**.

Theoretical prediction of the formation of trimers is schematically summarized in Figure 9.

***3.2.3. Formation Mechanism of 2,4′:2′,3″:2″,4‴-Tetraindolyl* 7.** Formation of 5,5′,5″,5‴,6,6′,6″,6‴-octahydroxy-2,4′:2′,3″:2″,4‴-tetraindolyl **7** was proposed to reflect a reaction of **2** against one of its two-electron-oxidants, extended quinone methide with geometry *Z* **12a**, i.e., **7** may be formed via the nucleophilic attack of the C2 position on the 4-substituted indole of **2** to the C3 position on the 2-substituted indole of **12a**.[19] In the following, we confirm the proposed reaction scheme theoretically.

The four tautomers of 2,4′-biindolyl **2a**−**2d** (Figure 10) were optimized in aqueous solution. We report in Table 7 energy

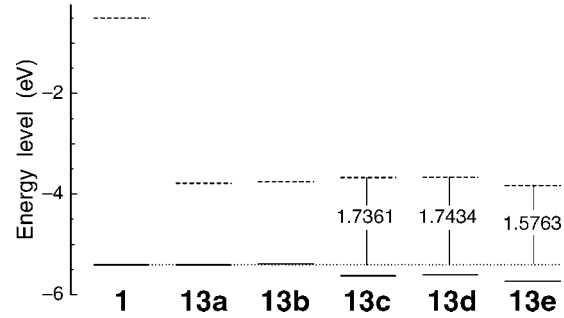

Figure 8. Energy level scheme of HOMO (horizontal solid line) and LUMO (horizontal dashed line) for **1** and **13**. The energy differences between $\varepsilon_{HOMO,1}$ and $\varepsilon_{LUMO,13c-13e}$ are also shown. This scheme indicates that **1** hardly reacts with **13a** and **13b** due to exchange repulsion and reacts as a nucleophile with **13c**−**13e** as electrophiles, and that the changes in the reactions of **1** against **13c**−**13e** are not so significant energetically.

levels of HOMO and LUMO of **2** to study the reaction picture, in which the probability of finding each molecule is also shown (for **12a**, see Table 3). The relation $\varepsilon_{HOMO,12a} < \varepsilon_{HOMO,2} < \varepsilon_{LUMO,12a} < \varepsilon_{LUMO,2}$ holds, and $\varepsilon_{LUMO,12a} - \varepsilon_{HOMO,2}$ is nearly constant. Therefore, we may conclude that **2** acts as a nucleophile and **12a** as an electrophile in the formation of **7** as proposed previously.[19]

The effective point charge and condensed Fukui function for **2**, which are needed to evaluate the general-purpose reactivity indicator, are summarized in Table 8. Analogous to the above-mentioned discussion, an approximation of $|\Delta N| = 1$ is probably reasonable from comparison of chemical formulas of **2**, **12a**, and **7**.

Analogous to the formation mechanism of the dimers and trimers, it seems reasonable to consider the limit of the electron-transfer-controlled reaction, $\kappa = -1$. We have shown $\Xi_{\Delta N=-1,\alpha}^{\kappa=-1}$ of each reactive position α for **2** in Table 8. As for the κ-dependence of reaction index, see the Supporting Information. Because **7** is formed only in the presence of Zn^{2+} ion,[19] the effect of Zn^{2+} on the reaction should be taken into account. Analogous to the formation process of **4** mentioned before, we may consider that Zn^{2+} ions reduce the reactivity of negatively charged reactive positions. Probably the effect will be larger at the positions with more negative charge. Conversely, Zn^{2+} ions will have no effect on the reactivity of positively charged positions. The C2 position on the 4-substituted indole of **2d** has the most negative $\Xi_{|\Delta N|=1,\alpha}^{\kappa=-1}$ among the five positively charged reactive positions of **2** and **12a** (for **12a**, see Table 4) and so it may be considered to be the key reactive position. We would like to mention that among the reactive positions of

TABLE 6: Effective Point Charges,[a] Condensed Fukui Function,[a] and Reactive Indicator[b] on Each Reactive Position for 13a−13d

		C3	C4	C7	C2′	C3′	C4′
13a	$q_\alpha^{(0)}$	− 0.1159	− 0.1284	− 0.2587	0.0783	− 0.0964	− 0.0991
	$q_\alpha^{(+)}$	− 0.2465	− 0.1849	− 0.2658	0.0373	− 0.1243	− 0.1727
	f_α^+	0.1306	0.0565	0.0071	0.0410	0.0278	0.0735
	$\Xi_{\Delta N=1,\alpha}^{\kappa=-1}$	−0.2613	−0.1130	−0.0142	−0.0820	−0.0557	−0.1471
13b	$q_\alpha^{(0)}$	− 0.0687	− 0.1587	− 0.2368	0.0943	− 0.0933	− 0.0996
	$q_\alpha^{(+)}$	− 0.1494	− 0.1723	− 0.2595	0.0363	− 0.1397	− 0.1730
	f_α^+	0.0806	0.0136	0.0227	0.0580	0.0464	0.0734
	$\Xi_{\Delta N=1,\alpha}^{\kappa=-1}$	−0.1613	−0.0272	−0.0454	−0.1161	−0.0928	−0.1468
13c	$q_\alpha^{(0)}$	− 0.2332	− 0.2883	− 0.2234	0.0905	− 0.1690	− 0.1992
	$q_\alpha^{(+)}$	− 0.2337	− 0.3545	− 0.3007	0.0463	− 0.1699	− 0.2425
	f_α^+	0.0005	0.0662	0.0773	0.0442	0.0008	0.0432
	$\Xi_{\Delta N=1,\alpha}^{\kappa=-1}$	−0.0010	−0.1324	−0.1546	−0.0883	−0.0017	−0.0865
13d	$q_\alpha^{(0)}$	− 0.1861	− 0.2887	− 0.1928	0.0741	− 0.1621	− 0.1650
	$q_\alpha^{(+)}$	− 0.1987	− 0.3467	− 0.2735	0.0283	− 0.1506	− 0.2581
	f_α^+	0.0126	0.0580	0.0807	0.0458	− 0.0116	0.0931
	$\Xi_{\Delta N=1,\alpha}^{\kappa=-1}$	−0.0253	−0.1160	−0.1613	−0.0916	0.0231	−0.1862

[a] In units of elementary charge. [b] Under the condition of $\Delta N = 1$ and $\kappa = -1$.

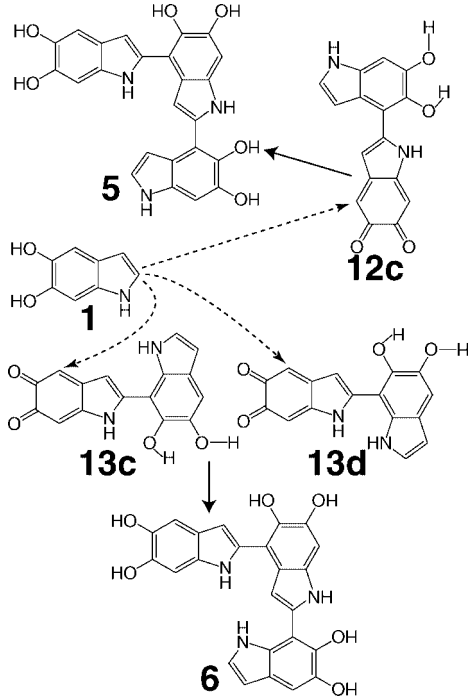

Figure 9. Proposed formation mechanism of 2,4′:2′,4″- and 2,4′:2′,7″-terindolyls. The nucleophilic attack of the C2 position of **1** to the C4 position on the 2-substituted indole of **12c** leads to **5** and that to the C4 position on the 2-substituted indole of **13c** or **13d** leads to **6**.

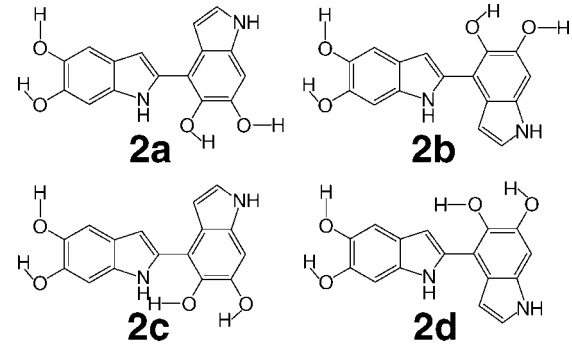

Figure 10. Structural formulas of the four 2,4′-biindolyls **2a**−**2d**.

TABLE 7: Energies of HOMO and LUMO for 2[a] and Probabilities of Finding Tautomer 2[b]

	2a	**2b**	**2c**	**2d**
ε_{HOMO}	−5.0306	−5.0412	−5.1116	−5.1223
ε_{LUMO}	−1.0740	−1.0225	−1.0838	−1.0786
probability	57.16	20.35	13.22	9.28

[a] In units of eV. [b] In units of %.

2a−**2d** the C2 position on 4-substituted indole for each molecule is the only position which is positively or small-negatively charged with larger negative $\Xi_{\Delta N=-1,\alpha}^{\kappa=-1}$. With respect to possible reactive positions of **12a**, the most negative $\Xi_{\Delta N=1,\alpha}^{\kappa=-1}$ is achieved at the C3 position on the 2-substituted indole. Fortunately, the effective point charge on the position is small negative and so it is reasonable to consider that the influence of Zn^{2+} ions on the position is not so significant. Therefore, we may theoretically conclude that **7** is formed via the nucleophilic attack of the C2 position on the 4-substituted indole of **2d** to the C3 position on the 2-substituted indole of **12a** in the presence of Zn^{2+} ions. This reaction is diagrammatically shown in Figure 11, and is basically consistent with the previous speculation[19] that **12a** or **12b** undergoes nucleophilic attack at the C3 position by **2** via the C2 position on the 4-substituted indole.

What are possible tetramers resulted from the coupling of **2** and **12** in the absence of transition-metal cations? In subsection 2, we found that a method taking account of both the value of $\Xi_{\Delta N,\alpha}^{\kappa}$ and Coulomb interaction between radical ions is preferable to explain product analysis of trimers consistently. Therefore, we adopt the method using values of $\Xi_{|\Delta N|=1,\alpha}^{\kappa=-1}$, $q_\alpha^{(-)}$, and $q_\alpha^{(+)}$ tabulated in Tables 4 and 8. It is natural to consider the case that Coulomb interaction between a reactive position on a radical cation and one on a radical anion is attractive and both reactive positions have large negative $\Xi_{|\Delta N|=1,\alpha}^{\kappa=-1}$. In this case, possible linkages are the linkage between the C2 position on the 4-substituted indole of **2c** and **2d** and the C3 position on the 2-substituted indole of **12a** and **12b** and that between the C2 position on the 4-substituted indole of **2c** and **2d** and the C7 position on the 4-substituted indole of **12a** and **12b**. As another possibility, we may consider the case that each of reactive positions on a radical cation and a radical anion has fully large negative $\Xi_{|\Delta N|=1,\alpha}^{\kappa=-1}$ and Coulomb interaction between them is repulsion but small enough. In this case, possible linkages are the linkage between the C7 position on the 4-substituted indole of **2** and the C7 position on the 4-substituted indole of **12a** and **12b**; that between the C3 position on the 2-substituted indole of **2a**, **2b**, and **2d** and the C7 position on the 4-substituted indole of **12a** and **12b**; and that between the

TABLE 8: Effective Point Charges,[a] Condensed Fukui Function,[a] and Reactive Indicator[b] on Each Reactive Position for 2

		C3	C4	C7	C2′	C3′	C7′
2a	$q_\alpha^{(0)}$	−0.2718	−0.2219	−0.1450	0.0743	−0.1704	−0.2061
	$q_\alpha^{(-)}$	−0.1238	−0.1482	−0.1535	0.1382	−0.1141	−0.0822
	f_α^-	0.1480	0.0737	−0.0085	0.0639	0.0563	0.1240
	$\Xi_{\Delta N=-1,\alpha}^{\kappa=-1}$	−0.2961	−0.1474	0.0170	−0.1278	−0.1127	−0.2480
2b	$q_\alpha^{(0)}$	−0.2419	−0.2160	−0.1376	0.0713	−0.1354	−0.2347
	$q_\alpha^{(-)}$	−0.0880	−0.1573	−0.1180	0.1451	−0.1120	−0.0958
	f_α^-	0.1540	0.0587	−0.0195	0.0738	0.0234	0.1390
	$\Xi_{\Delta N=-1,\alpha}^{\kappa=-1}$	−0.3079	−0.1174	−0.0391	−0.1476	−0.0468	−0.2779
2c	$q_\alpha^{(0)}$	−0.2043	−0.2036	−0.1418	0.0661	−0.1619	−0.1756
	$q_\alpha^{(-)}$	−0.1316	−0.1476	−0.1307	0.1768	−0.1194	−0.0317
	f_α^-	0.0727	0.0560	−0.0111	0.1107	0.0424	0.1439
	$\Xi_{\Delta N=-1,\alpha}^{\kappa=-1}$	−0.1453	−0.1119	−0.0222	−0.2213	−0.0848	−0.2877
2d	$q_\alpha^{(0)}$	−0.2292	−0.2187	−0.0974	0.0658	−0.1440	−0.1768
	$q_\alpha^{(-)}$	−0.0677	−0.1344	−0.1386	0.1887	−0.1362	−0.0676
	f_α^-	0.1615	0.0843	−0.0413	0.1229	0.0078	0.1091
	$\Xi_{\Delta N=-1,\alpha}^{\kappa=-1}$	−0.3230	−0.1686	0.0825	−0.2458	−0.0156	−0.2183

[a] In units of elementary charge. [b] Under the condition of $\Delta N = -1$ and $\kappa = -1$.

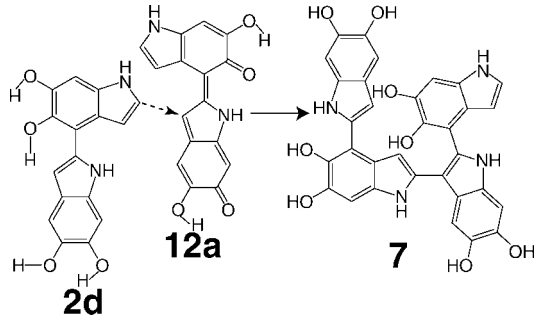

Figure 11. Proposed formation mechanism of 2,4′:2′,3″:2″,4‴-tetraindolyl in the presence of Zn^{2+}. The nucleophilic attack of the C2 position on the 4-substituted indole of **2d** to the C3 position on the 2-substituted indole of **12a** leads to **7**.

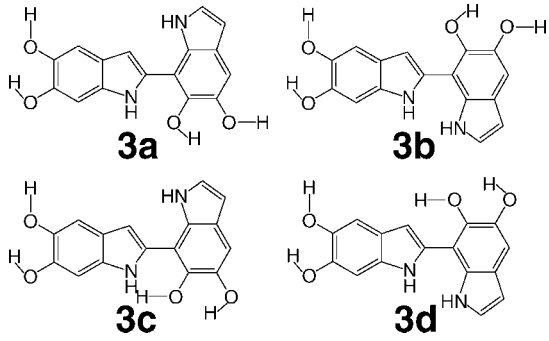

Figure 12. Structural formulas of the four 2,7′-biindolyls **3a**−**3d**.

C3 position on the 2-substituted indole of **2b** and **2d** and the C3 position on the 2-substituted indole of **12b**. Thus, theoretically predicted products are 2,4′:2′,3″:2″,4‴-, 2,4′:2′,7″:4″,2‴-, 2,4′:7′,7″:4″,2‴-, 2,4′:7′,3″:2″,4‴-, and 4,2′:3′,3″:2″,4‴-tetraindolyls.

3.2.4. Possible Tetramers via the Coupling of 2,7′-Biindolyl and Its Two-Electron-Oxidant. Possible tetramers resulted from the coupling of **3** (Figure 12) and **13** in the absence of transition-metal cations are as follows: The four tautomers of 2,7′-biindolyl **3a**−**3d** were optimized in aqueous solution. The HOMO and LUMO energies of **3**, which are tabulated with the probability of finding each tautomer in Table 9, should be compared with those of **13** to study the reaction picture (for **13**, see Table 5). The relation $\varepsilon_{HOMO,13} < \varepsilon_{HOMO,3} < \varepsilon_{LUMO,13} < \varepsilon_{LUMO,3}$ holds, and $\varepsilon_{LUMO,13} - \varepsilon_{HOMO,3}$ is nearly constant. Thus, we may conclude that **3** acts as a nucleophile and **13** as an electrophile in the coupling of **3** and **13**. In this reaction, it is probably

TABLE 9: Energies of HOMO and LUMO for *3*[a] and Probabilities of Finding Tautomer *3*[b]

	3a	**3b**	**3c**	**3d**
ε_{HOMO}	−5.1141	−5.1289	−5.2224	−5.2688
ε_{LUMO}	−1.0262	−0.9627	−1.0347	−0.9666
probability	59.82	24.11	8.95	7.13

[a] In units of eV. [b] In units of %.

reasonable to consider the condition of $|\Delta N| = 1$ and $\kappa = -1$. The effective point charge, condensed Fukui function, and reactive indicator under the condition of $\Delta N = -1$ and $\kappa = -1$ on each reactive position for **3** are summarized in Table 10 (for **13**, see Table 6). For the dependence of the reactive indicators on κ for **3**, see the Supporting Information.

Analogous to the above-mentioned discussion, we first consider the case of attractive Coulomb interaction between reactive positions on a radical cation and a radical anion. The most possible linkage is the linkage between the C2 position on the 7-substituted indole of **3c** and the C3 position on the 2-substituted indole of **13a**. In the case of small enough repulsion Coulomb interaction, possible linkages are the linkage between the C3 position on the 2-substituted indole of **3b** and **3d** and the C3 position on the 2-substituted indole of **13a** and **13b**; that between the C4 position on the 7-substituted indole of **3** and the C3 position on the 2-substituted indole of **13a** and **13b**; and that between the C4 position on the 7-substituted indole of **3** and the C4 position on the 7-substituted indole of **13a** and **13b**. Therefore, 2,7′:2′,3″:2″,7‴-, 7,2′:3′,3″:2″,7‴-, 2,7′:4′,3″:2″,7‴-, and 2,7′:4′,4″:7″,2‴-tetraindolyls are predicted theoretically as possible products via the coupling of **3** and **13**.

Quite recently, Pezzella et al.[20] succeeded in isolating three tetramers from the four above-predicted tetramers, 7,2′:3′,3″:2″,7‴-, 2,7′:4′,4″:7″,2‴-, and 2,7′:2′,3″:2″,7‴-tetraindolyls (**8**, **9**, and **10**), by the oxidation of **3**. This suggests that the present theoretical prediction is reasonable. Possible formation paths of the isolated tetramers by the oxidation of **3** in the absence of transition-metal cations are summarized in Figure 13. It was also shown that **10** becomes preferable enough to be one of the major products in the presence of Zn^{2+} ion. They consider that this is caused by the increase in the reactivity of the C2 position on the 7-substituted indole of **3** by the influence of Zn^{2+} ion.[20] The increase in the reactivity of that position may be explained theoretically as already discussed before in this paper: The influence of Zn^{2+} ion is not so significant for positions with positive charge. Zn^{2+} ions more strongly reduce the reactivity

TABLE 10: Effective Point Charges,[a] Condensed Fukui Function,[a] and Reactive Indicator[b] on Each Reactive Position for 3

		C3	C4	C7	C2′	C3′	C4′
3a	$q_\alpha^{(0)}$	−0.2508	−0.2173	−0.1581	0.0418	−0.1688	−0.2527
	$q_\alpha^{(-)}$	−0.1377	−0.1594	−0.1214	0.0847	−0.1014	−0.1188
	f_α^-	0.1131	0.0579	0.0368	0.0429	0.0674	0.1339
	$\Xi_{\Delta N=-1,\alpha}^{\kappa=-1}$	−0.2263	−0.1158	−0.0735	−0.0858	−0.1348	−0.2678
3b	$q_\alpha^{(0)}$	−0.2486	−0.2145	−0.1298	0.0697	−0.1879	−0.2714
	$q_\alpha^{(-)}$	−0.0880	−0.1659	−0.1003	0.0764	−0.1054	−0.1475
	f_α^-	0.1606	0.0486	0.0295	0.0067	0.0825	0.1239
	$\Xi_{\Delta N=-1,\alpha}^{\kappa=-1}$	−0.3212	−0.0971	−0.0590	−0.0134	−0.1650	−0.2478
3c	$q_\alpha^{(0)}$	−0.2097	−0.1959	−0.1340	0.0584	−0.1679	−0.2307
	$q_\alpha^{(-)}$	−0.1163	−0.1687	−0.1134	0.1262	−0.1346	−0.0946
	f_α^-	0.0934	0.0272	0.0206	0.0679	0.0333	0.1361
	$\Xi_{\Delta N=-1,\alpha}^{\kappa=-1}$	−0.1868	−0.0543	−0.0412	−0.1357	−0.0666	−0.2722
3d	$q_\alpha^{(0)}$	−0.2251	−0.2040	−0.1395	0.0741	−0.1819	−0.2223
	$q_\alpha^{(-)}$	−0.0766	−0.1441	−0.1284	0.1245	−0.1270	−0.1104
	f_α^-	0.1485	0.0599	0.0111	0.0504	0.0549	0.1119
	$\Xi_{\Delta N=-1,\alpha}^{\kappa=-1}$	−0.2969	−0.1198	−0.0221	−0.1009	−0.1098	−0.2238

[a] In units of elementary charge. [b] Under the condition of $\Delta N = -1$ and $\kappa = -1$.

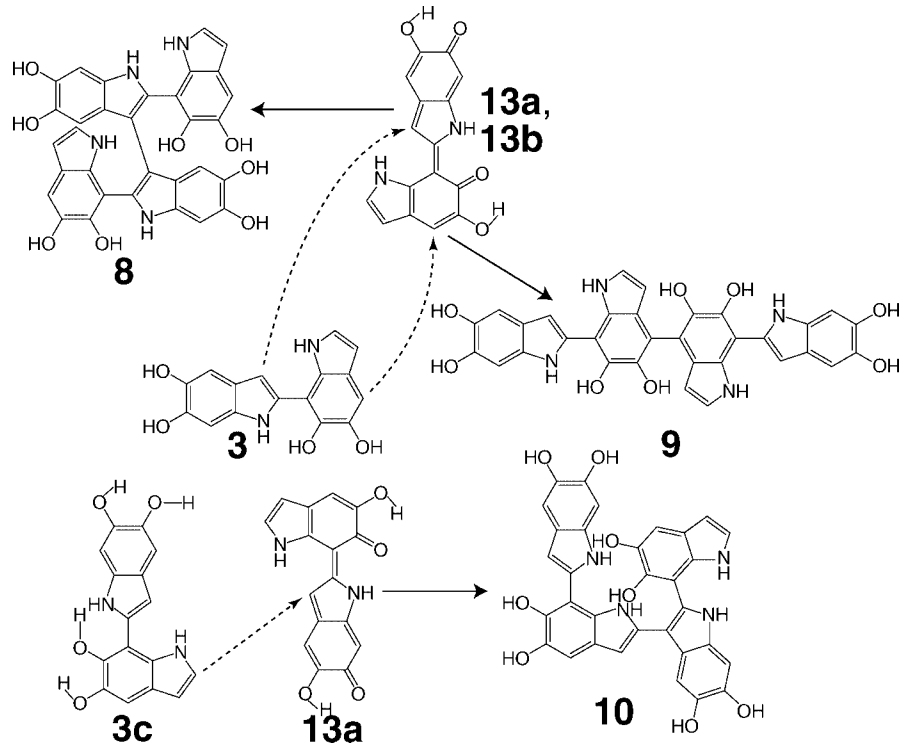

Figure 13. Proposed origin of the formations of the isolated tetramers, 7,2′:3′,3″:2″,7‴-, 2,7′:4′,4″:7″,2‴-, and 2,7′:2′,3″:2″,7‴-tetraindolyls. The nucleophilic attack of the C3 position on the 2-substituted indole of **3** to the C3 position on the 2-substituted indole of **13a** or **13b** leads to **8**; that of the C4 position on the 7-substituted indole of **3** to the C4 position on the 7-substituted indole of **13a** or **13b** leads to **9**; and that of the C2 position on the 7-substituted indole of **3c** to the C3 position on the 2-substituted indole of **13a** leads to **10**. Note that for the reaction paths of forming **8** and **9**, we predict that **8** and **9** are the results of the reactions of **3** against **13a** and **13b**. However, the structural formula only of **13a** is shown as a typical molecule for the reactions forming **8** and **9** in this scheme (top picture).

at the positions with the larger negatively charge. For **3**, the effective point charge of the C2 position on the 7-substituted indole is positive and the other reactive positions are negative (see Table 10). Therefore, the reactivity of the C2 position on the 7-substituted indole of **3** relatively increases.

4. Summary

We have studied the oxidative polymerization mechanism of DHI with the general-purpose reactivity indicator from ab initio density-functional theory calculations. Theoretical predictions may explain reasonably the experimental results. It has been demonstrated that the polymerization up to tetramers is the electron-transfer-controlled reaction in contrast to the previous speculation that the reaction is dominated by the electrostatic interaction. We have also concluded that the electrostatic interaction may play a regioselective important role in the reactant complex.

It has been found that the general-purpose reactivity indicator used herein is literally general-purpose but not a panacea. In the present case, effective point charges on reactive positions of radical ions work well as a complementary indicator, too.

As for dimerization, the following has been shown. Four conformers of DHI, **1a**−**1d**, participate in the reaction as a nucleophile while IQ predominantly participates as an electrophile among three tautomers. The C2 position of DHI is the most reactive among the reactive positions of DHI and IQ. The

isolated dimers, 2,4′- and 2,7′-biindolyls, are formed via the nucleophilic attack of the C2 position of DHI to the C4 and C7 positions of IQ as an electrophile. The C3 position of IQ is much less reactive. The 2,2′-biindolyl is considered to be formed as a result of transition-metal cations reducing the reactivity of the negatively charged positions, i.e., the C3, C4, and C7 positions both of DHI and IQ.

In the trimer formation process, reactions between the most stable and next-most stable two-electron-oxidants of 2,4′- and 2,7′-biindolyls and DHI are ruled out because of steric hindrance. These two-electron-oxidants of dimers are rather consumed to form tetramers. This finding may explain why such polymerization mechanism as a dimer–dimer coupling may occur in the oxidation of DHI. The reaction of DHI against the third stable two-electron-oxidant of 2,4′-biindolyl, 2-substituted quinone with *sp* symmetry, is considered to form 2,4′:2′,4″-terindolyl via the nucleophilic attack of the C2 position of DHI to the C4 position on the 2-substituted indole of 2-substituted quinone with *sp* symmetry, and the reaction of DHI against the third or fourth stable two-electron-oxidant of 2,7′-biindolyl, 2-substituted quinone with *sp* symmetry or 2-substituted quinone with *ap* symmetry, may form 2,4′:2′,7″-terindolyl with almost the same reaction for 2,4′:2′,4″-terindolyl. Here, 2,4′:2′,7″-terindolyl has been explained theoretically not by using only the general-purpose reactivity indicator but by considering the effective point charges of radical ions in the reaction intermediate state.

The formation of tetramer involves a dimer–dimer coupling because the most stable and next-most stable two-electron-oxidants of 2,4′-biindolyl are not consumed in forming trimers. The formation of isolated 2,4′:2′,3″:2″,4‴-tetraindolyl is reasonably explained by the nucleophilic attack of the C2 position on the 4-substituted indole of 2,4′-biindolyl to the C3 position on the 2-substituted indole of extended quinone methide with geometory *Z* under the condition that Zn^{2+} reduces the reactivity of the position with large-negative point charge. As products resulted from the oxidation of dimers in the absence of transition-metal cations, 2,4′:2′,3″:2″,4‴-, 2,4′:2′,7″:4″,2‴-, 2,4′:7′,7″:4″,2‴-, 2,4′:7′,3″:2″,4‴-, and 4,2′:3′,3″:2″,4‴-tetraindolyls may be formed from the oxidation of the 2,4′-biindolyl, and 2,7′:2′,3″:2″,7‴-, 7,2′:3′,3″:2″,7‴-, 2,7′:4′,4″:7″,2‴-, and 2,7′:4′,3″:2″,7‴-tetraindolyls from the oxidation of 2,7′-biindolyl. The former three of the four predicted tetramers for the oxidation of 2,7′-biindolyl were isolated quite recently. This seems to validate the present theoretical prediction.

The present work opens doors to identifying oligomer structures of melanin not a priori but logically according to the reactivity of its precursors. This is a significant advance in modeling melanin structure.

Supporting Information Available: The excitation energies of **1**, **11**, **12**, **13**, **2**, and **3**, the reactivity of **11b** and **11c**, ΔN in forming dimers, trimers, and tetramers, and κ -dependence of $\Xi^{\kappa}_{|\Delta N| = 1, \alpha}$ for **1**, **11**, **12**, **13**, **2**, and **3**. This material is available free of charge via the Internet at http://pubs.acs.org.

References and Notes

(1) See, for example (a) Wakamatsu, K.; Ito, S. *Pigment Cell Res.* **2002**, *15*, 174–183, and references cited therein.

(2) Pezzella, A.; Vogna, D.; Prota, G. *Tetrahedron* **2002**, *58*, 3681–3687.

(3) Ito, S. *Pigment Cell Res.* **2003**, *16*, 230–236.

(4) Pezzella, A.; Vogna, D.; Prota, G. *Tetrahedron: Asymmetry* **2003**, *14*, 1133–1140.

(5) Hennessy, A.; Oh, C.; Diffey, B.; Wakamatsu, K.; Ito, S.; Rees, J. *Pigment Cell Res.* **2005**, *18*, 220–223.

(6) Nighswander-Rempel, S. P.; Riesz, J.; Gilmore, J.; Bothma, J. P.; Meredith, P. *J. Phys. Chem. B* **2005**, *109*, 20629–20635.

(7) Liu, Y.; Hong, L.; Wakamatsu, K.; Ito, S.; Adhyaru, B.; Cheng, C. Y.; Bowers, C. R.; Simon, J. D. *Photochem. Photobiol.* **2005**, *81*, 135–144.

(8) d'Ischia, M.; Napolitano, A.; Pezzella, A.; Land, E. J.; Ramsden, C. A.; Riley, P. A. *Adv. Heterocycl. Chem.* **2005**, *89*, 1–63.

(9) Meredith, P.; Sarna, T. *Pigment Cell Res.* **2006**, *19*, 572–594.

(10) McGinness, J. *Science* **1972**, *177*, 896–897.

(11) Wolbarsht, M. L.; Wash, A. W.; George, G. *Appl. Opt.* **1981**, *20*, 2184–2186.

(12) McGinness, J.; Corry, P.; Proctor, P. *Science* **1974**, *183*, 853–855.

(13) Tran, M. L.; Powell, B. J.; Meredith, P. *Biophys. J.* **2006**, *90*, 743–752.

(14) Riesz, J. J.; Gilmore, J. B.; McKenzie, R. H.; Powell, B. J.; Pederson, M. R.; Meredith, P. *Phys. Rev. E* **2007**, *76*, 021915.

(15) Pezzella, A.; Napolitano, A.; d'Ischia, M.; Prota, G. *Tetrahedron* **1996**, *52*, 7913–7920.

(16) Napolitano, A.; Corradini, M. G.; Prota, G. *Tetrahedron Lett.* **1985**, *26*, 2805–2808.

(17) d'Ischia, M.; Napolitano, A.; Tsiakas, K.; Prota, G. *Tetrahedron* **1990**, *46*, 5789–5796.

(18) Napolitano, A.; Crescenzi, O.; Prota, G. *Tetrahedron Lett.* **1993**, *34*, 885–888.

(19) Panzella, L.; Pezzella, A.; Napolitano, A.; d'Ischia, M. *Org. Lett.* **2007**, *9*, 1411–1414.

(20) Pezzella, A.; Panzella, L.; Natangelo, A.; Arzillo, M.; Napolitano, A.; d'Ischia, M. *J. Org. Chem.* **2007**, *72*, 9225–9230.

(21) Stark, K. B.; Gallas, J. M.; Zajac, G. W.; Eisner, M.; Golab, J. T. *J. Phys. Chem. B* **2003**, *107*, 3061–3067; **2003**, *107*, 11558−11562.

(22) Stark, K. B.; Gallas, J. M.; Zajac, G. W.; Golab, J. T.; Gidanian, S.; McIntire, T.; Farmer, P. J. *J. Phys. Chem. B* **2005**, *109*, 1970–1977.

(23) Pezzella, A.; Panzella, L.; Crescenzi, O.; Napolitano, A.; Navaratman, S.; Edge, R.; Land, E. J.; Barone, V.; d'Ischia, M. *J. Am. Chem. Soc.* **2006**, *128*, 15490–15498.

(24) Kaxiras, E.; Tsolakidis, A.; Zonios, G.; Meng, S. *Phys. Rev. Lett.* **2006**, *97*, 218102.

(25) Anderson, J. S. M.; Melin, J.; Ayers, P. W. *J. Chem. Theory Comput.* **2007**, *3*, 358–374; **2007**, *3*, 375−389.

(26) Parr, R. G.; Yang, W., *Density-Functional Theory of Atoms and Molecules*; Oxford University Press: New York, 1989.

(27) Koch, W.; Holthausen, M. C., *A Chemist's Guide to Density Functional Theory*, 2nd ed.; Wiley-VCH: Weinheim, Germany, 2001.

(28) Becke, A. D. *J. Chem. Phys.* **1993**, *98*, 5648–5652.

(29) Petersson, G. A.; Bennett, A.; Tensfeldt, T. G.; Al-Laham, M. A.; Shirley, W. A.; Mantzaris, J. *J. Chem. Phys.* **1988**, *89*, 2193–2218.

(30) Clark, T.; Chandrasekhar, J.; Spitznagel, G. W.; Schleyer, P. V. R. *J. Comput. Chem.* **1983**, *4*, 294–301.

(31) Cammi, R.; Mennucci, B.; Tomasi, J. *J. Phys. Chem. A* **2000**, *104*, 5631–5637.

(32) Breneman, C. M.; Wiberg, K. B. *J. Comput. Chem.* **1990**, *11*, 361–373.

(33) Frisch, M. J.; Trucks, G. W.; Schlegel, H. B.; Scuseria, G. E.; Robb, M. A.; Cheeseman, J. R.; Montgomery, J. A., Jr.; Vreven, T.; Kudin, K. N.; Burant, J. C.; Millam, J. M.; Iyengar, S. S.; Tomasi, J.; Barone, V.; Mennucci, B.; Cossi, M.; Scalmani, G.; Rega, N.; Petersson, G. A.; Nakatsuji, H.; Hada, M.; Ehara, M.; Toyota, K.; Fukuda, R.; Hasegawa, J.; Ishida, M.; Nakajima, T.; Honda, Y.; Kitao, O.; Nakai, H.; Klene, M.; Li, X.; Knox, J. E.; Hratchian, H. P.; Cross, J. B.; Bakken, V.; Adamo, C.; Jaramillo, J.; Gomperts, R.; Stratmann, R. E.; Yazyev, O.; Austin, A. J.; Cammi, R.; Pomelli, C.; Ochterski, J. W.; Ayala, P. Y.; Morokuma, K.; Voth, G. A.; Salvador, P.; Dannenberg, J. J.; Zakrzewski, V. G.; Dapprich, S.; Daniels, A. D.; Strain, M. C.; Farkas, O.; Malick, D. K.; Rabuck, A. D.; Raghavachari, K.; Foresman, J. B.; Ortiz, J. V.; Cui, Q.; Baboul, A. G.; Clifford, S.; Cioslowski, J.; Stefanov, B. B.; Liu, G.; Liashenko, A.; Piskorz, P.; Komaromi, I.; Martin, R. L.; Fox, D. J.; Keith, T.; Al-Laham, M. A.; Peng, C. Y.; Nanayakkara, A.; Challacombe, M.; Gill, P. M. W.; Johnson, B.; Chen, W.; Wong, M. W.; Gonzalez, C.; Pople, J. A. Gaussian 03, revision C.02; Gaussian, Inc.: Wallingford, CT, 2004.

(34) Il'ichev, Y. V.; Simon, J. D. *J. Phys. Chem. B* **2003**, *107*, 7162–7171.

JP711025M